Clays and Clay Minerals, Vol. 44, No. 3, 398–407, 1996.

ANGLE-RESOLVED X-RAY PHOTOELECTRON STUDIES OF CLEAVAGE IN CHLORITES

STEPHEN EVANS AND ANTHONY G. HIORNS†

Electron Spectroscopy Laboratory, Institute of Earth Studies, University of Wales
Aberystwyth, Dyfed, SY23 3DB, U.K.

Abstract—The cleavage of two single-crystal chlorites (a clinochlore and a penninite) has been studied using angle-resolved X-ray photoelectron spectroscopy (XPS). Both minerals cleaved in regions not typical of the bulk; the composition of the clinochlore was found to be especially non-uniform. The brucitic interlayer divided evenly between the pair of new surfaces exposed for two cleaves in the clinochlore, but was partitioned unequally in two cleaves in the penninite. The differences in apparent composition between the complementary pairs of surfaces are interpreted to show a marked preference of octahedral Al for the brucitic layer, in agreement with X-ray bulk structure refinements. For both chlorites, the layer charge was reduced in regions of easy cleavage, which also had a higher proportion of Si and less tetrahedral Al than the bulk chlorite. The percentages of tetrahedral aluminium deduced from the XPS surface analyses agreed satisfactorily with the percentages independently determined by consideration of the magnitude of anisotropy in the X-ray photoelectron diffraction (XPD) patterns. The XPD patterns from the clinochlore for rotation about axes parallel and antiparallel to the crystallographic a-axis were identical, showing that tetrahedral ordering was absent.

Key Words—Chlorite, Cleavage, ESCA, Photoelectron, Structure, XPS.

INTRODUCTION

There has recently been renewed interest in the structures of the surfaces of the sheet silicates with the advent of atomic-force microscopy (Henderson et al. 1994; Vrdoljak et al. 1994). Impressively, surface structures can now be mapped almost atom by atom. However, information on atomic identities is not so readily achieved, and the element-specific surface spectroscopies still have an important role to play. Over a number of years we have pioneered the use of angle-resolved X-ray photoelectron spectroscopy (XPS) in studies of the micas, developing new routes to the characterization of cation ordering patterns (Adams et al. 1978; Evans et al. 1979a; Ash et al. 1987, 1988). The information obtained from XPS strictly relates only to the outermost few repeat units of the crystals, although for many micas there has been evidence indicating that the surface and bulk compositions are closely similar. In these cases, therefore, it has been reasonable to infer bulk characterization from that at the surface. However, for samples of phlogopite, vermiculite and lithium biotite, cleavage was found to occur most readily in regions of high Al content (Evans et al. 1979a, 1979b) while a lepidolite has been shown to cleave preferentially in manganese-enriched regions (Evans and Raftery 1982).

In this paper, we extend these studies to chlorites. The information obtainable from X-ray photoelectron diffraction (XPD) is limited because of the additional complexity of the chlorite structure, but we have found that, uniquely, cation-ordering information can be obtained from the angle-integrated XPS surface analyses. This possibility arises because the crystallographic repeat distance is comparable with the XPS sampling depth, and the whole unit cell is therefore not always uniformly sampled. Chlorites comprise a mica-like 2:1 sheet silicate component with a brucite-like interlayer, making the overall repeat distance perpendicular to the layers as much as ~14 Å. The unit cell vectors within the layers are a ~5.4 Å (parallel to the mirror plane) and b ~9.3 Å (perpendicular to the mirror plane), as for the micas. The principal issues we have been able to address are: 1) whether chlorites, like micas, tend to cleave in regions of anomalous (non-bulk) composition, and how the brucitic interlayer is distributed between two newly-created cleavage surfaces; 2) whether either of the principal octahedral cations (Mg^{2+}, Al^{3+}) has a detectable preference for this brucitic interlayer; and 3) whether Si and Al occupy the tetrahedral sites randomly or in an ordered fashion.

EXPERIMENTAL AND DATA PROCESSING

Two chlorite crystals from the museum collection of the University College of North Wales, Bangor, were studied. The first was pale green (nearly colorless), originally from Tyrol, Austria and was described as clinochlore (specimen reference number 8236). The other sample, which was dark green in color and from Zermatt, Switzerland, was described as penninite (specimen reference number 8237). Both were of sufficient area for easy XPS analysis (that is, greater than

† Present address: English China Clays International, John Keay House, St. Austell, Cornwall.

~14 × 6 mm) and thick enough at several mm, to yield several cleavage surfaces for examination.

Initial X-ray characterization using a low-power diffractometer (Teltron Ltd) showed nine (00*l*) reflections in the range n = 3 to n = 16 for each sample, yielding values of 14.1 Å for the layer spacings of the clinochlore and 14.3 Å for the penninite. Transmission Laue photographs of the two specimens revealed a mirror plane for each specimen, parallel to the a-axis of the 2:1 layers in the chlorite structure, thus enabling the axis of rotation in the XPD experiments to be selected.

Fragments from both samples were finely ground and analyzed by conventional procedures starting with sodium hydroxide fusion. Silicon was determined gravimetrically as quinoline silicomolybdate; aluminium gravimetrically as the 8-hydroxyquinolate; iron colorimetrically as the 1,10-phenanthroline complex and magnesium by atomic absorption using standard additions, following Bennett and Reed (1971). The Al determinations were found to be so low as to be clearly erroneous, and unfortunately, insufficient material remained for repeat determinations. However, the X-ray layer spacings can be used to estimate the tetrahedral Al content. By using the plot of Deer, Howie and Zussman (1962) and assuming the sum of the cation charges to be 28, as for the surface analyses to be described below, the following best estimates for the bulk formula were obtained:

Clinochlore: $(Si_{2.7}Al_{1.3})(Al_{1.5}Fe^{II}_{0.25}Mg_{4.1}\square_{0.15})O_{10}(OH)_8$

Penninite: $(Si_{3.3}Al_{0.7})(Al_{0.8}Fe^{II}_{0.28}Mg_{4.9})O_{10}(OH)_8$

Angle-resolved XPS data sets were collected using a modified AEI/Kratos ES200A electron spectrometer under semi-automatic microcomputer control (Evans and Elliott 1982). The crystals were cleaved in air using a razor blade and mounted onto a copper probe tip by two small stainless steel screws, with the desired axis of rotation aligned parallel to the axis of the probe. Most of the data were collected with the axis of rotation parallel or antiparallel to the b-axis, at right angles to the Laue mirror plane, but data for the clinochlore were also collected for the first cleave for rotation about axes parallel and antiparallel to the a-axis. Seven different cleavage surfaces, distinguished later by the letters A–G, were examined for the clinochlore. All were from the same crystal. D and E were a pair of surfaces ("complementary surfaces") exposed by the same cleavage process, as were F and G. In all, thirteen data sets were collected for the clinochlore, including two duplicate sets (surface B) obtained after remounting the crystal, to confirm that the data were satisfactorily reproducible. Four surfaces were examined for the penninite, comprising two pairs of complementary surfaces denoted H, I and J, K. Again, duplicate data sets were collected for surfaces H and I to confirm reproducibility. Thus, ten data sets were collected in total for this specimen.

In each data set, the regions of interest from the Mg Kα photoelectron spectra (O1s, Cl, and a region including Si2s, Al2s, Si2p, Mg2s, Al2p and Mg2p) were recorded at 3.75° angular intervals over the maximum accessible range of electron takeoff angle, θ, giving approximately 23 sets of spectra for each rotation axis, as detailed by Ash et al. (1988). The Fe signals (Fe2p) were too weak to yield adequate signal/noise but some spectra were recorded nevertheless so that an estimate of the iron concentration at the surface could be obtained. The equilibrium surface charge on the specimens under X-irradiation (typically 3–4 eV) varied somewhat with angle, but was never large enough to cause any difficulties for data processing or interpretation.

The spectra comprising each full data set were smoothed by convolution with a Gaussian function of 2 eV full-width-at-half-maximum (Evans and Hiorns 1986) to optimize the signal/noise ratio. The net heights above background were then computed and plotted using interactive FORTRAN77 programs on a 486/33 IBM-compatible PC as described by Ash et al. (1988) to provide XPD patterns, that is, plots of normalized ratios between peak intensities as a function of electron takeoff angle.

These ratio plots are independent of the instrumental angular response function, and therefore more reproducible; but for some purposes the individual elemental angular dependences are required. The instrumental variation of sensitivity with angle, which is critically dependent on probe position, must then be compensated. However, for samples such as these, with many different crystallographic sites, the background underlying the XPS peaks, which is made up of inelastically scattered photoelectrons from within the sample, retains no significant diffraction modulation with the electron takeoff angle. The integrated intensity of the background (summed over the whole energy range recorded) then provides a good indication of the relative sensitivity of the instrument under the conditions used, and the intensities of individual peaks recorded at different angles can be normalized by division by this background intensity, as discussed by Ash et al. (1988). This procedure was adopted whenever the variation of individual intensities with angle was required.

Because all core photoelectron signals, of similar kinetic energy, which derive from equivalent sites have indistinguishable angular anisotropies, Si2s and Si2p data could be summed, as were Mg2s and Mg2p, to provide improved reproducibility in the plots. The essential constancy of the Si2s/Si2p and Mg2s/Mg2p intensity ratios was first checked for each data set. Random variations of ±5% were typical, as in previous studies (Ash et al. 1987, 1988; Evans et al. 1979a;

Table 1. Mean XPS surface analyses for all the chlorite cleavages examined.

Mineral	Surface[2]	Comment[3]	Nos. of cations[1] in formula $^{IV}M_4{}^{VI}M_6O_{10}(OH)_8$					
			^{IV}Si	^{IV}Al	^{VI}Al	^{VI}Mg	^{VI}Fe4	□
Clinochlore	A	Mean from four data sets (2 ± *a*-axis and 2 ± *b*-axis), consistent to 1%	3.14	0.86	1.54	3.84	0.29	0.33
Clinochlore	B	Mean from four data sets (2 pairs ± *b*-axis), consistent to 1%	3.53	0.47	1.58	3.56	0.32	0.54
Clinochlore	C	Single data set only	3.61	0.39	1.47	3.66	0.33	0.54
Clinochlore	D, E	Mean from complementary surfaces, *b*-axis; consistent to 1%	3.10	0.90	1.49	3.95	0.28	0.28
Clinochlore	F, G	Mean from complementary surfaces, *b*-axis	3.70	0.30	1.31	3.86	0.34	0.49
Penninite	H	Mean of four data sets from same surface (2 pairs ± *b*-axis), consistent to 3%; complementary to next entry.	3.56	0.44	1.21	4.12	0.30	0.37
Penninite	I	Mean of four data sets from same surface (2 pairs ± *b*-axis), consistent to 1%; complementary to above.	3.70	0.30	1.31	3.88	0.31	0.50
Penninite	J	Single data set, *b* axis, complementary to next entry.	3.56	0.44	1.15	4.19	0.30	0.36
Penninite	K	Single data set, *b*-axis, complementary to above.	3.51	0.49	1.18	4.18	0.29	0.35

[1] Derived from the mole ratios obtained from the XPS peak areas (see note 3) by: 1) normalizing so that the sum of the charges on the detected cations becomes 28, for charge balance against $O_{10}(OH)_8$; 2) assigning all the Si and as much of the Al as required to fill all the tetrahedral sites; and 3) then assigning the balance of the cations to the octahedral sites. Since there are fewer than 10 cations for the 28 positive charges, there are octahedral vacancies, indicated by □, in all the surface formulae. The octahedral sites in the 2:1 layer and in the brucitic interlayer are not distinguished in this procedure.

[2] Surfaces A–G were exposed by cleavage of one crystal of the clinochlore, and surfaces H–K similarly for a single crystal of the penninite. The four pairs D, E; F, G; H, I; and J, K are complementary surfaces exposed by one cleavage process each.

[3] Each XPD data set comprised ~23 spectra for each peak. The Si and Mg analyses were derived from both the 2s and the 2p peaks, Al from Al2s only, using the procedures described by Evans et al. (1978) and Evans et al. (1979b). The symbol ± denotes experimental rotation axes parallel and antiparallel to the crystallographic direction specified.

[4] Assumed to retain bulk concentration (relative to Si) at the cleavage. In data sets where Fe2p was included, a value comparable with the bulk composition was obtained. An accurate XPS analysis cannot, however, be obtained, partly because the Fe peaks are too weak and partly because the presence of satellite peaks makes the true area virtually impossible to define. Because the amount of Fe is relatively small, however, even a 50% underestimation makes relatively little difference to the derived formulae.

Evans and Raftery 1982). For Al, only the 2s peak could be used because the 2p peak is heavily overlapped by the major component of the Mg KLL Auger emission.

Surface analytical information was also obtained from the same data. The scattered-electron background mentioned above was subtracted as described by Ash et al. (1988), the area of each peak for each spectrum was computed, and the ionization cross-section data of Evans et al. (1978) applied to yield an apparent composition for each angle. These apparent compositions were averaged over the whole angular range. Compositions obtained in this way are effectively angle-integrated, and are not affected by the diffraction modulation evident in all such data from single crystals (Evans et al. 1979b).

RESULTS AND DISCUSSION

Surface analytical data are given in Table 1 for all the surfaces examined. The individual peak areas had statistical uncertainties (Evans 1992) within the range 0.4–5%, and the resulting mean analyses (based on 23 or 46 peaks, that is, one or two peaks for each element at each angle) should thus have a statistical error no greater than ~1%. The scatter on nominally-identical data in the Table confirms an overall analytical precision of this order. Systematic errors may be larger, possibly as much as 5% (Evans et al. 1978), but will affect all the data similarly.

1. The Distribution of the Brucitic Interlayer Between Complementary Cleavage Surfaces

The brucitic interlayer normally carries a significant positive charge, balancing the negative charge on the 2:1 layers, and it would be expected to be divided between the two new surfaces produced when the crystal is cleaved. However, because XPS is surface-sensitive on a similar scale to the chlorite repeat depth the inelastic mean free path (λ) of the faster photoelectrons is about 20 Å (Seah and Dench 1979), compared with a 14 Å crystallographic repeat distance XPS can be used, almost uniquely, to establish how the interlayer is actually partitioned between the two cleavage surfaces. In the recent atomic-force microscopy experiments reported by Vrdoljak et al. (1994) this issue was not addressed, apparently because dif-

ferent imaging techniques had to be applied to resolve the brucitic and 2:1 layers.

The chlorite repeat is made up of 10 sheets of atoms (O, M^{IV}, O, M^{VI}, O, M^{IV}, O, O, M^{VI}, O). If the uppermost surface were the 2:1 layer, XPS signals from each successive sheet into the crystal, at depth d_i, would be progressively attenuated by a factor $\exp(-d_i/\lambda\cos\theta)$, and the brucitic layer, well below the surface, would contribute less than proportionally to the total XPS signal. Conversely, if the surface terminated in a complete brucitic layer, the 2:1 layer would contribute less. A FORTRAN77 computer program was written to calculate the apparent compositions for any actual chlorite composition and angular range of measurement, and for any assumed distribution of the interlayer between the two cleavage surfaces. If the reasonable assumption is made that the true mean composition is uniform through the region in which cleavage has occurred, a difference between the apparent compositions for each side indicates that the brucitic layer divided unevenly on cleavage, and the mean of the two apparent compositions is an excellent approximation to the true composition. If exactly half the interlayer remains on each new surface, the two analyses are the same and the indicated composition is not significantly different from the actual composition. For the angular range used for the XPD data, the limiting cases of 'no brucitic layer on the surface' and 'a complete brucitic layer on the surface' yield Si analyses (normalized as in Table 1) approximately 10% higher and 10% lower than the actual composition, with a near-linear dependence in between. This is not significantly affected by the assumed octahedral Al, Mg, Fe distribution, because all the Si is in the tetrahedral sites of the 2:1 layer. Thus, whenever two complementary surfaces from the same cleavage yield different Si surface analyses, we can immediately deduce what fraction of the interlayer adheres to each surface. Two pairs of complementary cleaves were examined for each chlorite (Table 1) and it was found that for both the penninite pairs, the Si analyses did indeed differ, to extents indicating a 60%/40% split (surfaces H, I) and 53.5%/46.5% (surfaces J, K) in the other. The percentages obtained depend to some extent on the electron inelastic mean free path used in the calculations. The values given are for a typical value of 20 Å (Seah and Dench 1979). If this parameter were as large as 34 Å, as suggested by Evans et al. (1979a), the degree of inequality increases by about half (to 65%/35% for surfaces H, I), but none of the subsequent interpretation is affected.

The two complementary pairs (D, E and F, G) for the clinochlore showed no significant difference. However, these two cleaves for this crystal do reveal a large non-uniformity in composition, and although the range of Si analyses for the remainder of the surfaces (A–C) is of the right order to be explained as a consequence of an uneven interlayer distribution it would seem unwise to pursue the interpretation, since it is clear that the composition is variable over distances of the order of millimeters. However, if the variation between surfaces A and B were due to uneven layer distribution, the concomitant differences in apparent Al and Mg analyses would lead to qualitatively identical conclusions as the parallel changes seen for the penninite, surfaces H–K, as discussed below.

2. Characterization of Cation Ordering Between the 2:1 and Brucitic Layers From Surface Analyses

Initially, the computer program was set up to assign the same Al occupancy in the brucitic layer as in the tetrahedral sites of the 2:1 layer (following, arbitrarily, one conventional view of the expected charge balance in chlorites), placing the remaining Al in the octahedral sites of the 2:1 layer and dividing the octahedral vacancies equally between the layers. However, this assignment did not reproduce the observed Mg and Al variation between complementary surfaces. In both complementary pairs of penninite surfaces, high Si was accompanied by low Al. This implied that the Al was concentrated within the brucitic layer, and by progressively transferring Al from the 2:1 layer to the brucitic layer in the assumed compositions until the observed degree of difference was reproduced, estimates of the Al distribution could be obtained. To match the indicated Mg analyses, it was then necessary to transfer Mg from the brucitic layer into the 2:1 layer. The final result was a chlorite structural formula for each pair of complementary surfaces, with Al and Mg partitioned between the two layers, and the outermost brucitic layer unequally divided between the two surfaces created by the cleavage. This reproduced all the experimental analyses for both new surfaces to within ~0.4% on average, with no instance of disagreement greater than 2%. These formulae are given in Table 2. It should be emphasized that the method is not very sensitive to small changes in cation distribution, and the distribution of the iron and the vacancies was, to some extent, arbitrary, so that a range of compositions centered on those quoted would still be in acceptable agreement with the experiment. The acceptable range would bracket changes in the layer charge of at least 0.2 units. However, since a charge of +1.0 on the brucitic interlayer is believed to be the most stable arrangement (Bailey 1988), and both the formulae in Table 2 show values well below this figure, these results still suggest that the regions of easy cleavage are ones in which local compositional variations have significantly reduced the layer charge. For the cleavage yielding surfaces H, I in particular, even if all the brucitic vacancies were filled by transferring iron from the talc sites, the layer charge could only increase to +0.57.

Table 2. The cation ordering in penninite revealed by XPS surface analyses.

Surfaces[2]	Nos. of cations[1] in formula $^{IV}M_4{}^{VI}M_6O_{10}(OH)_8$									
	IV_{Si}	IV_{Al}	VI_{Al} (talc)	VI_{Mg} (talc)	$VI_{Fe}{}^{3}$ (talc)	□[4] (talc)	VI_{Al} (brucitic)	VI_{Mg} (brucitic)	□[4] (brucitic)	Layer charge[5]
H, I	3.62	0.38	0.68	1.82	0.30	0.20	0.57	2.19	0.24	0.09
J, K	3.54	0.46	0.00	2.58	0.30	0.12	1.17	1.61	0.22	0.72

[1] Calculated from the apparent compositions given in Table 1 by means of the computer program described in the text. These structural formulae, combined with the unequal partitioning of the brucitic interlayer on cleavage deduced from the differing Si XPS analyses for the pairs of complementary surfaces, reproduced all the apparent compositions for these surfaces in Table 1 to within <2% (mean 0.4%) for all elements.

[2] The surface labels are the same as in Table 1. The pairs H, I and J, K are complementary (exposed by the same cleavage process).

[3] In the absence of any XPD data for Fe, this element has been arbitrarily assigned to the talc-like sites.

[4] The distribution of the vacancies (□) is, to some extent, arbitrary. Transferring Fe into the brucitic layer would increase the vacancy concentration in the talc layer, reduce it in the brucitic layer, and increase the layer charge. However, in the refined bulk structures given by Bailey (1988) a preference for Fe occupying brucitic sites is always accompanied by a higher brucitic vacancy concentration.

[5] The layer charge, calculated from the structural formula given, is positive on the brucitic layer and negative on the talc-like (2:1) layer.

The observed preference of Al for the brucitic layer is entirely in line with crystallographic data for bulk chlorites. Of the nine Mg-dominant trioctahedral chlorite structure refinements tabulated by Bailey (1988), 5 have all their octahedral Al in the brucitic layer, 3 have the great majority brucitic and only in one instance, does the octahedral Al in the 2:1 layer reach 60% of the content of the brucitic layer. The fact that for surfaces H, I there is not an even greater concentration of Al in the brucitic layer thus reinforces the comment above about the probability of cleavage in regions of low layer charge. The ratio between brucitic Mg content and Mg in the 2:1 layer varies between 0.67 and 1.04 in Bailey's table, with 8 of the 9 structures between 0.67 and 0.76. Thus, our surfaces J, K are not markedly atypical (0.62) in this respect. Surfaces H, I are more unusual with a ratio of 1.17.

3. Compositional Differences Between Surface and Bulk

It is notable that the great majority of the analyses in Table 1 show substantially more Si than typical chlorite formulae. Foster (1962) found a range of 2.34 to 3.45 of the 4 tetrahedral sites occupied by Si, while Bailey and Brown (1962) reported a range of 2.30 to 3.39, mean 2.69. All but 2 of the entries in Table 1 are above this range. Since the XPS analyses are normalized to a sum of cation charges of 28, and it seems certain that systematic errors in the analytical procedure are <5% for Si, Mg and Al, this is unlikely to be an experimental artefact. For example, to restore the Si content of the most Si-rich surfaces (F, G) to Foster's highest figure of 3.45 would require there to have been 0.93 undetected divalent cations (equivalent to 26% of the Mg detected) or 0.62 trivalent cations per formula unit (41% of the Al detected), levels that are inconceivably high. The possibility that a number of elements could be present at low concentration, and hence remain undetected, was eliminated by consideration of the XPS O1s intensities. The number of oxygen atoms detected in the cleaved surfaces was always within a few percent of that expected for the cations detected in a chlorite (that is, ... $O_{10}(OH)_8$) framework. The point is reinforced by consideration of the Si/Mg mole ratios. For low-iron chlorites this ratio is consistently in the range 0.60 to 0.68. All 8 such chlorites in the table by Bailey (1988) cited above and both our samples (bulk analysis) lie within these limits. Yet the surfaces in Table 1 show mean values of 0.91 for the clinochlore and 0.87 for the penninite. Since Si carries the highest charge of all the cations in chlorite, charge balance requires excess Si to be accompanied either by an excess of low-valent cations (Mg or Fe), not the case here, or by an increased concentration of octahedral vacancies. A local concentration of these vacancies in the brucitic layer could contribute markedly to a reduction in the layer charge (even below the estimates in Table 2, in which the vacancies are distributed between the layers), with consequent easier cleavage. The available structure refinements (Bailey 1988) suggest that, when vacancies are present in the bulk, a higher concentration in the brucitic layer than in the 2:1 layer is not uncommon.

4. Interpretation of the Photoelectron Diffraction Patterns

Three examples of the XPD patterns obtained from these chlorites are reproduced in Figures 1–3. Statistical uncertainties (Evans 1992) on the net heights were typically 2% and generally less than 5%, and the scatter of the data from the diagrams is generally of this order. A complete set of patterns, including individual peak intensities as well as ratios, for the surfaces identified as A, B, H and I can be found in Hiorns (1991).

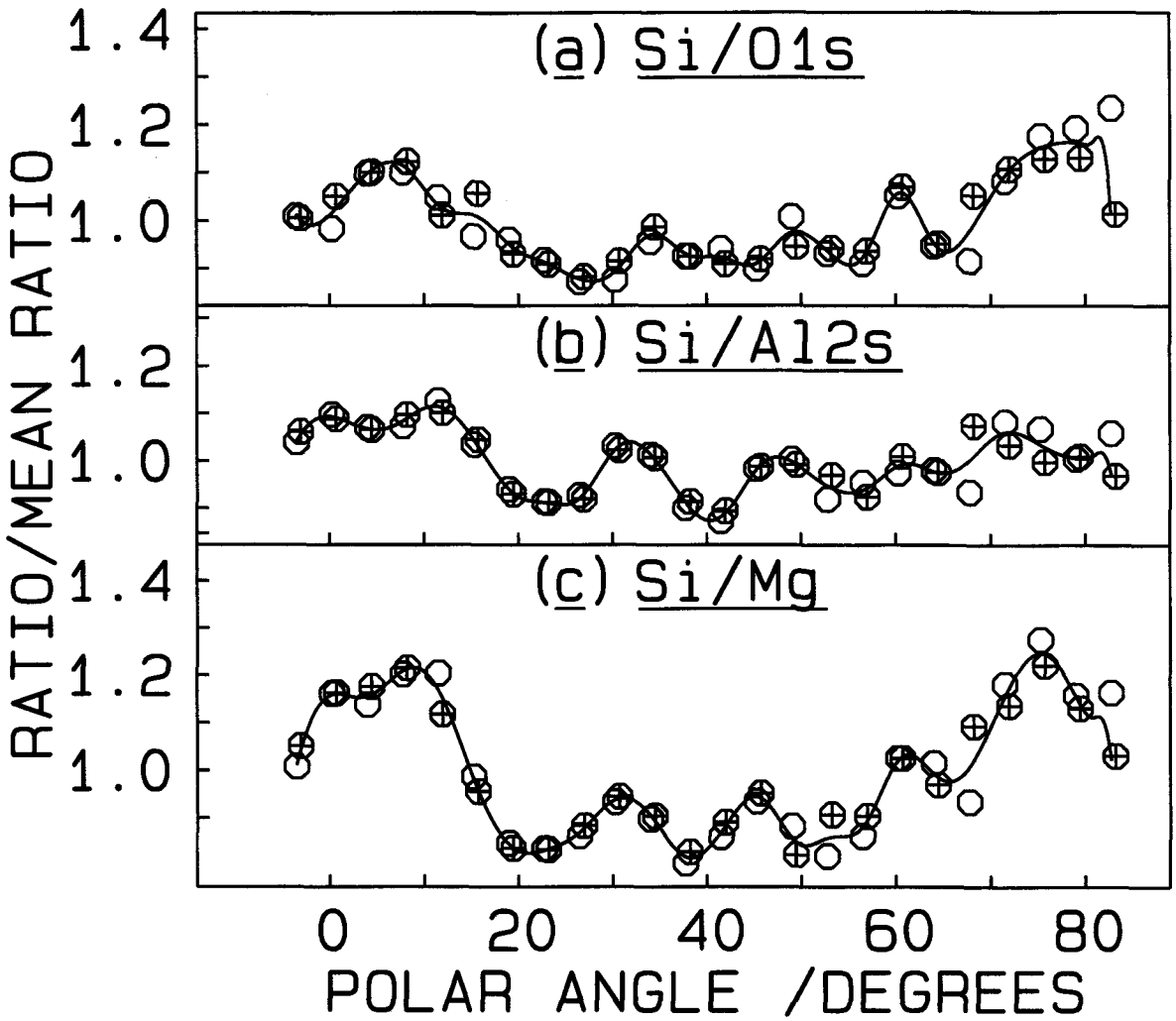

Figure 1. XPD patterns for the clinochlore for rotation about axes parallel and antiparallel to the a-axis, plotted on the same axes (surface A). The labels Si and Mg represent the sums of data from the 2s and 2p peaks.

The XPD patterns from different surfaces varied somewhat in the general magnitudes of the angular anisotropy, far more than was found for the micas. This probably reflects greater disorder in the chlorites, associated with damage to the partitioned interlayer at the surface. The patterns illustrated for the clinochlore (Figures 1 and 2) are typical, whereas those for the penninite (Figure 3) show the greatest anisotropies. However, all the surfaces gave patterns for the same rotation axes showing qualitatively similar features.

A detailed interpretation of these XPD patterns is more difficult than it was for the micas (Ash et al. 1987) because of the multiplicity of possible octahedral sites when all the possibilities for cation ordering are taken into account. However, some conclusions can be drawn simply by considering the symmetry properties of the patterns.

TETRAHEDRAL CATION ORDERING. Consider Figure 1 first. If tetrahedral ordering of the Si and Al into alternate sites were to be present, the two rotations about the a-axis would not yield equivalent results, and it is clear from the diagram that any differences are within experimental error. We conclude that tetrahedral ordering is not present in this clinochlore, which is in agreement with all modern chlorite X-ray structure refinements (Bailey 1988). Such ordering has once been reported in chlorite (Steinfink 1958) but that refinement is now discounted (Bailey 1988).

THE POSSIBLE ROLE OF STACKING FAULTS IN PROMOTING CLEAVAGE. The remaining XPD data all relate to rotation about directions parallel to the crystallographic b-axis (Figures 2 and 3). Throughout, the patterns for rotation about the b-direction in one orientation are different from those obtained after the crystal has been

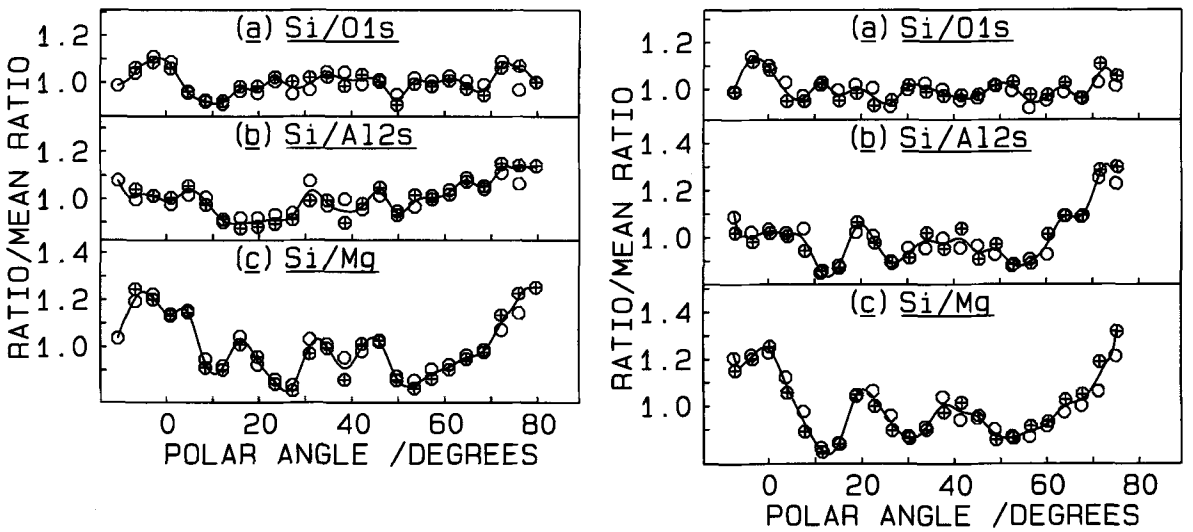

Figure 2. XPD patterns for the clinochlore for rotation about axes parallel (left) and antiparallel (right) to the b-axis. The two symbol types distinguish duplicate data sets, both from surface B. Data from surface A were closely similar, but with greater anisotropy. The labels Si and Mg represent the sums of data from the 2s and 2p peaks.

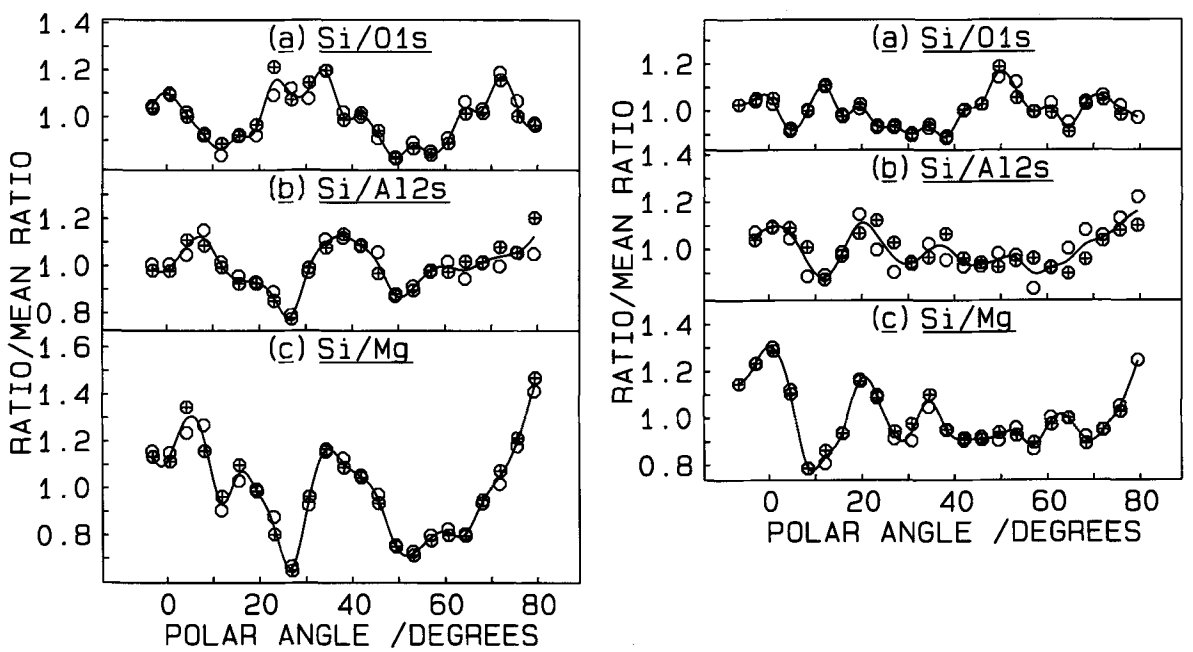

Figure 3. XPD patterns for the penninite for rotation about axes parallel (left) and antiparallel (right) to the b-axis. The two symbol types distinguish duplicate data sets, both from surface I. This surface showed the greatest angular anisotropy of all those studied; angular variations for complementary surface H were noticeably smaller. The labels Si and Mg represent the sums of data from the 2s and 2p peaks.

rotated through 180° (shown on the left and right of Figures 2 and 3). This is, of course, expected from consideration of the symmetry of the 2:1 layers. We can make immediate use of this distinction. In all 4 cases where complementary pairs of surfaces were examined, the correlation between the b-axis XPD patterns showed that the orientation of the 2:1 sheet was the same on each side of the cleave. A change in the normal stacking order of the 2:1 layers is not a factor in promoting facile cleavage.

OCTAHEDRAL CATION ORDERING. The patterns for the two chlorites show many similarities, but also distinct differences, which can be seen by comparing Figures

2 and 3. The compositions are not so different that such marked effects would be expected to arise either from bond length and angle differences or from scattering-factor differences. Throughout the large compositional variations from cleave to cleave, the patterns for each mineral remain distinctive. Similar observations from early mica XPD studies (Evans and Raftery 1982) were later explained (Ash et al. 1988) as a consequence of differing patterns of ordering in the octahedral sites, and this seems likely to be the case here also. However, a great deal more data would be required from additional experimental rotation axes to confirm the hypothesis. Given that ordering could occur here in either or both the octahedral sheets full characterization would probably still not prove possible in the absence of a theoretical framework adequate to predict patterns for any given postulated structure.

COMPARISON WITH MICA XPD PATTERNS. The b-axis patterns for Si/Mg and Si/O in particular are superficially similar to those from biotite mica (Ash et al. 1988), which is not unexpected given the similarity of the Si environment and the fact that about half the Mg in chlorite also has a mica-like environment. Only about half of the outermost brucitic layer will be present, so that the XPD pattern may be dominated by the outer 2:1 layer. The "buried" interlayer beneath the 2:1 layer would then contribute relatively little because of the exponential attenuation of signals from below the surface. The increased repeat distance relative to the micas is not important because most of the XPD structure is generated by elastic scattering from atoms quite close to the emitter. The Si/Mg patterns from a vermiculite (d_{001} also ~14 Å) without interlayer Mg are thus virtually identical to those of other micas (Evans et al. 1979a, 1979b). However, if both chlorites were of Bailey's Type I, with the octahedral slant in the interlayer parallel to that in the 2:1 layer, the nearest-neighbor directions surrounding the octahedral cations would be the same. This would be expected to give rise to marked similarities between the angular distributions for photoelectrons from the 2:1 octahedral sites and the brucitic octahedral sites. We consider this a much less probable explanation, since 80% of all chlorites are of Type II, in which the octahedral slants are opposed.

ENHANCED-FORWARD-SCATTERING INTERPRETATION OF THE DIFFRACTION MODULATION OF PEAK INTENSITIES. Some general features of even these complex XPD data can be qualitatively explained using the "enhanced forward scattering" concept introduced by Egelhoff (1984). The photoelectron intensity is enhanced when a near-neighbor atom lies directly in the electron emission direction. This effect is clearly visible for simple systems, but for complex crystals, such as the micas, interference effects often mask it. In Figure 4, we show normalized intensities for the individual elements. There is structure in the Mg and, to a lesser extent because of tetrahedral substitution, in the Al, angular distributions that has no parallel in the mica data of Ash et al. (1988). In particular, the strong peak at ~27°, variable in strength from surface to surface, must originate from the brucitic layer. It seems likely that this arises from enhanced forward scattering from the row of nearest-neighbor hydroxyl ions which would lie in the emission plane at approximately this angle. However, the weaker feature for the 180°-reversed rotation axis at ~11°, which is also absent from the corresponding mica data, has no obvious explanation. The 27°-feature is about half to two-thirds as intense in the Al curve, and this degree of attenuation is in accord with the Al distribution for this surface in Table 2: 55% of the Mg but only 35% of the Al is in the brucitic layer. One other feature of the curves in Figure 4 can be explained by the simple enhanced-forward-scattering concept. The Si and O intensities are maximal at 0°, and for all the Si atoms and many O atoms, this is a nearest-neighbor direction. Magnesium, in contrast, has no nearest neighbor in this direction and its emission intensity is consequently not maximal at this angle. A similar contrast occurs in the spinel structure between the tetrahedral and octahedral ion XPD (Ash and Evans 1993).

ESTIMATION OF THE PERCENTAGE OF TETRAHEDRAL ALUMINIUM FROM THE XPD PATTERNS. If the Al and Mg were distributed similarly between the various octahedral sites, the Si/Al patterns would merely be weaker copies of those for Si/Mg, because some of the Al occupies tetrahedral sites equivalent to those of Si and has the same angular dependence. The percentage by which the anisotropy is reduced would directly indicate the percentage of the Al in tetrahedral sites (Evans et al. 1979b). Since the Si/Mg and Si/Al patterns have quite similar profiles between approximately 10° and 50°, despite the Mg and Al having differing distributions between the 2:1 layer sites and the brucitic-layer sites, this should still represent a reasonable approximation. In Figure 5 we compare the percentages of tetrahedral Al estimated this way with those determined completely independently from the surface analysis for every surface for which at least two data sets exist. The agreement is generally good, with only the b-axis data for surfaces A and H, I seriously out of line. It is notable that both the highest (40–45%, surfaces A, and D, E) and the lowest (18%, surfaces F, G) percentages arise in surfaces from one specimen, the clinochlore. However, there is a clear tendency for the Si/Al2s XPD range to be reduced by more than the analyses would suggest. Several factors may contribute to this, including possible damage to the brucitic layer on cleavage. There are also clearly some differences between the Al and Mg curves, confirming

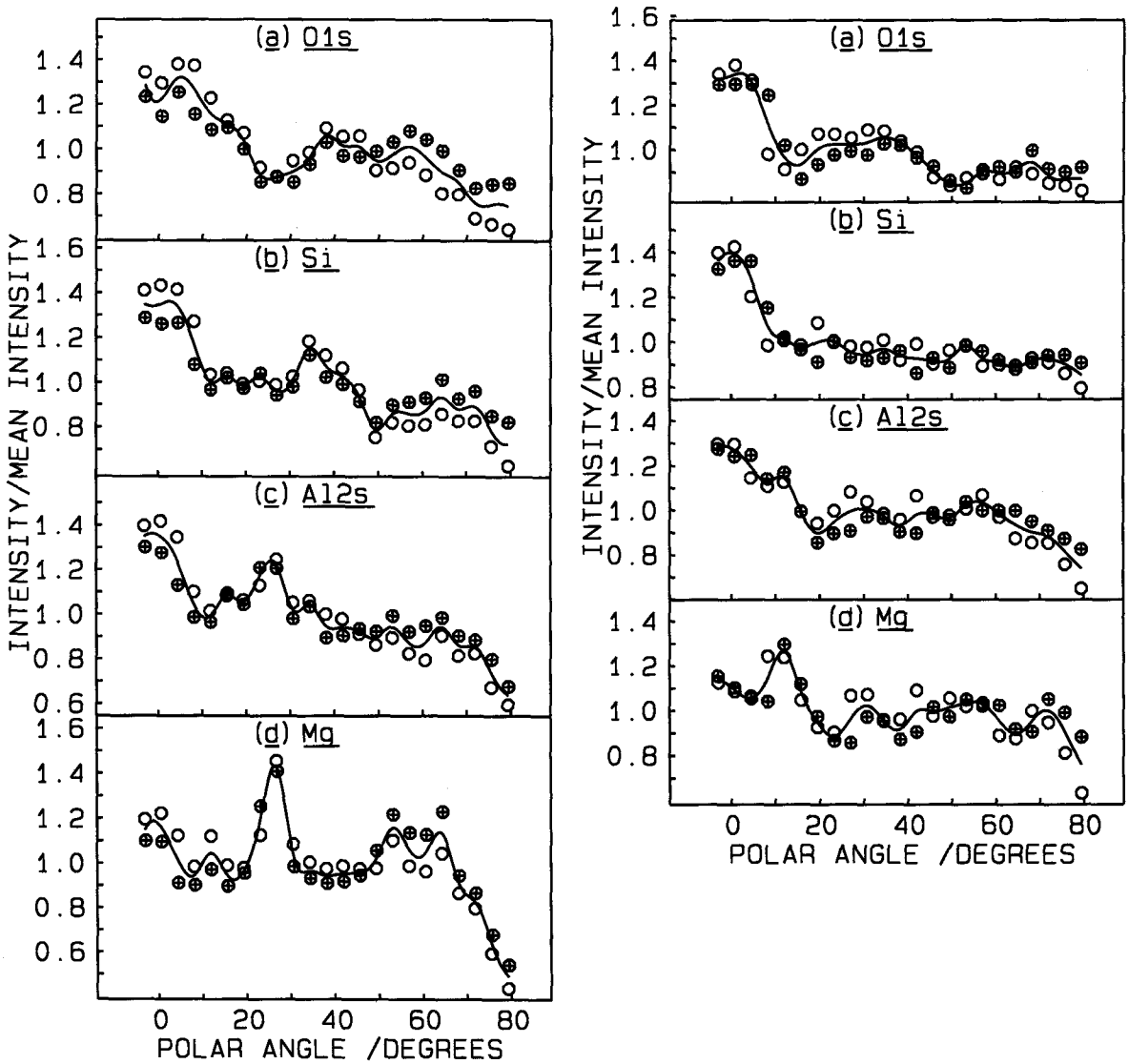

Figure 4. Angular dependence of individual peak intensities, approximately corrected for the instrumental angular response function, for the data used to compute Figure 3. The two symbol types distinguish duplicate data sets from the same surface, and the labels Si and Mg represent the sums of data from the 2s and 2p peaks.

the view based on the surface analyses that these ions are in fact distributed differently between the 2:1 layer and the interlayer. Different ordering within either layer could also be a factor.

CONCLUSIONS

The composition of chlorite crystals is—in the 2 specimens studied—markedly non-uniform in the direction perpendicular to the cleavage plane. The effects were more marked in the clinochlore than in the penninite. These compositional variations parallel effects reported in some, but by no means all, the micas previously studied. However, in the chlorites cleavage occurred preferentially in regions that were Si-rich (compared with Al- or Mn-rich in the micas), and therefore have an increased octahedral vacancy concentration. Characterization of the local structure at the cleavage was possible when the brucitic interlayer divided unequally on cleavage, so that the XPS analyses of the two surfaces produced were not the same. This only occurred for the penninite, where in one case as much as 60% of the brucitic interlayer adhered to one surface. Octahedral Al was found to exhibit a strong preference for the brucitic layer at the cleavage, as in previously-refined bulk structures, but there was also clear evidence for a reduced layer charge at the newly-exposed surface. The XPD data proved useful in confirming the low percentage of Al occupying tetrahedral sites, that

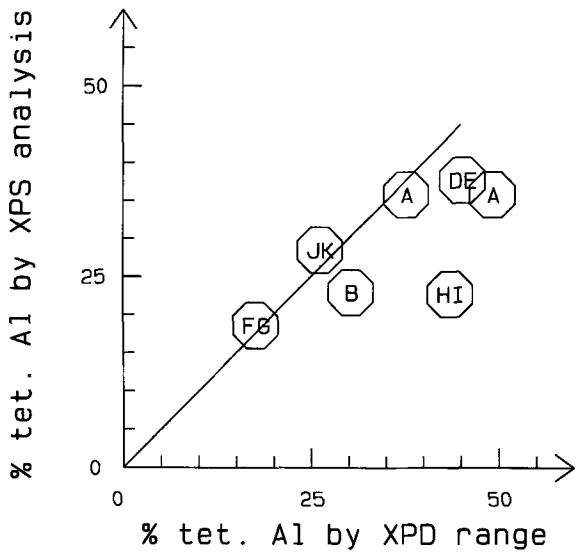

Figure 5. Comparison of the estimates of the percentage of Al in tetrahedral sites at chlorite surfaces obtained from the angular distributions in the photoelectron spectra (XPD) and from the angle-integrated XPS analyses. Surface labels are included in each point.

Mg and Al were distributed differently between the 2 layers, and the expected absence of tetrahedral Si, Al ordering.

ACKNOWLEDGMENTS

We thank the SERC for support under Standard Grant GR/C 64431 and for a Research Studentship (to AGH), the University College of North Wales, Bangor for samples, and C. Noli for experimental assistance in the later stages of the work.

REFERENCES

Adams JM, Evans S, Thomas JM. 1978. X-ray photoelectron diffraction: A new technique for structural studies of complex solids. J Am Chem Soc 100:3260–3262.

Ash LA, Evans S. 1993. X-ray photoelectron diffraction studies of the surface chemistry of non-stoichiometric synthetic spinel. Surf Interface Anal 20:1075–1080.

Ash LA, Evans S, Hiorns AG. 1987. Cation ordering in lepidolite and biotite studied by X-ray photoelectron diffraction. Clay Miner 22:375–386.

Ash LA, Clark SL, Evans S, Hiorns AG. 1988. X-ray photoelectron diffraction studies of the micas lepidolite and biotite. J Chem Soc, Dalton Trans 859–879.

Bailey SW. 1988. Chlorites: Structures and crystal chemistry. In:Mineralogical Society of America reviews in mineralogy 19:347–403.

Bailey SW, Brown BE. 1962. Chlorite polytypism: I Regular and semi-random one-layer structures. Am Mineral 47: 819–850.

Bennett H, Reed RA. 1971. Chemical methods of silicate analysis. London: Academic Press. p 73–79.

Deer WA, Howie RA, Zussman J. 1962. Rock forming minerals, Vol. 3, Sheet silicates. London: Longman. p 131–136.

Egelhoff WF. 1984. X-ray photoelectron and Auger-electron forward scattering—a new tool for studying epitaxial growth and core-level binding energy shifts. Phys Rev B 30:1052–1055.

Evans S. 1992. Estimation of the uncertainties associated with XPS peak intensity determination. Surf Interface Anal 18:323–332.

Evans S, Adams JM, Thomas JM. 1979a. The surface structure and composition of layered silicate minerals: Novel insights from X-ray photoelectron diffraction, K-emission spectroscopy and cognate techniques. Phil Trans R Soc Lond A 292:563–591.

Evans S, Elliott DA. 1982. Interfacing AEI/Kratos electron spectrometers to a microcomputer for data acquisition and processing. Surf Interface Anal 4:267–270.

Evans S, Hiorns AG. 1986. Convolutional smoothing algorithms in electron spectroscopy. Surf Interface Anal 8:71–73.

Evans S, Pritchard RG, Thomas JM. 1978. Relative differential subshell photoionisation cross-sections (Mg Kα) from lithium to uranium. J Electron Spectrosc Rel Phen 14: 341–358.

Evans S, Raftery E. 1982. X-ray photoelectron diffraction studies of lepidolite. Clay Miner 17:443–452.

Evans S, Raftery E, Thomas JM. 1979b. Angular variations in core-level XPS peak intensity ratios from single-crystal solids. Surf Sci 89:64–75.

Foster MD. 1962. Interpretation of the composition and a classification of the chlorites. U.S. Geol Surv Prof Paper 414-A:1–33.

Henderson GS, Vrdoljak GA, Eby RK, Wicks FJ, Rachlin AL. 1994. Atomic-force microscopy studies of layer silicate minerals. Coll Surf A—Physicochem Engineer Aspects 87:197–212.

Hiorns AG. 1991. Applications of electron spectroscopy in inorganic chemistry. [Ph.D. Thesis]. Aberystwyth: University of Wales. p 96–114.

Seah MP, Dench WA. 1979. Quantitative electron spectroscopy of surfaces: A standard data base for electron inelastic mean free paths in solids. Surf Interface Anal 1:2–19.

Steinfink H. 1958. The crystal structure of chlorite. I. A monoclinic polymorph. Acta Crystallog 11:191–195.

Vrdoljak GA, Henderson GS, Fawcett JJ, Wicks FJ. 1994. Structural relaxation of the chlorite surface imaged by the atomic-force microscope. Am Mineral 79:107–112.

(Received 10 January 1995; accepted 7 September 1995; Ms. 2605)